Sigma J Eng Nat Sci, Vol. 44, No. 4, pp. 2396–2414, August, 2026

Sigma Journal of Engineering and Natural Sciences
Web page info: https://sigma.yildiz.edu.tr
DOI: 10.14744/sigma.2026.2102

Research Article

Numerical modeling of seismic impacts on cistern structures

Pınar USTA EVCİ[1,*], Ayşe BÜYÜKÜNSAL[1], Neşe BOZKURT[1]

[1]*Isparta University of Applied Sciences, Isparta, 32200, Türkiye*

ARTICLE INFO

Article history
Received: 23 August 2024
Revised: 18 November 2024
Accepted: 13 January 2025

Keywords:
Cistern; Historical Building; Numerical Modelling; Time History Analyses

ABSTRACT

The present research constitutes a thorough investigation of the seismic characteristics of an 18th-century stone masonry cistern situated in the Fethiye area of Turkey, highlighting the need to protect cultural heritage structures located in areas vulnerable to seismic events. The mechanical characteristics of the stone masonry materials used for building the cistern were determined using experiments. The seismic behavior of the cistern was then analyzed both statically and dynamically using the software program SAP2000 V22. It can be observed from the analysis that the seismic response in the case of the cistern along the short axis is higher than in the case of the long axis. In addition, some important stress concentration points were revealed by the analysis, with the maximum compressive stress being 0.525 MPa and maximum tensile stress being 0.272 MPa. Moreover, the outside surface of the cistern experienced the maximum horizontal displacement of 1.5 cm along the short direction. Also, it was seen that shear stresses in wall A1, which contains the door opening, exceeded the typical shear stress of the wall, implying imminent risk of local failure. Stress concentration areas were found near the main openings of the dome and openings in walls, representing the key points that require interventions. In general, it can be inferred from the analysis that the structure withstands seismic events, but accumulated stress levels in certain areas can cause cracking. Some important recommendations on retrofitting have been provided based on the analysis, offering an opportunity to improve the structure's seismic response. Thus, the current research contributes to the field of analysis of seismic characteristics of historical masonry structures by providing an analysis of an important water storage structure. The study has been conducted in accordance with the objectives stated and provides important recommendations on how to retro-fit the structure, making it more resistant to seismic loads. While previous studies of historical masonry structures were mainly concerned with the analysis of their seismic responses, with buildings such as churches, mosques, and towers considered, very few researchers examined the cistern structures from the point of view of retrofitting in relation to seismic events.

Cite this article as: Usta Evci P, Büyükünsal A, Bozkurt N. Numerical modeling of seismic impacts on cistern structures. Sigma J Eng Nat Sci 2026;44(4):2396–2414.

***Corresponding author.**
*E-mail address: pinarusta@isparta.edu.tr

This paper was recommended for publication in revised form by Editor-in-Chief Ahmet Selim Dalkilic

Published by Yıldız Technical University Press, İstanbul, Turkey

INTRODUCTION

Since water is a crucial element for the existence of life, the supply and storage of water have been one of the main problems of the human being [1,2]. Throughout history, settlements were generally built near water. In the following periods, in settlements located on fertile lands but established far from water sources, structures were built to supply and collect water [2]. Aqueducts and waterways used for supply and cisterns used to collect water [3] were constructed as hydraulic structures in ancient times.

Cisterns, serving as fundamental hydraulic structures, were strategically positioned in various parts of ancient cities. Cisterns were common and varied from cities to caravanserais to countryside to ensure that rain water could be collected in accordance with different purposes during varying seasons of the year. This phenomenon is well described in the studies conducted by Demirci and Bilgin [1] and Oter [4], revealing the extent of importance given to cisterns in terms of water storage in ancient civilizations [5]. Cisterns were usually roofed structures since long periods of sun exposure tended to degrade water quality [6]. There were several techniques used to build cisterns, ranging from simple ones in the form of clay tanks to more complex constructions, such as underground reservoirs [5]. In Anatolia, especially countryside areas, cisterns were mostly built from stones [7]. Stone masonry is the earliest and most common construction technique. These structures are resistant to fire, water, and insect damage [8]. But stone masonry buildings are generally vulnerable to strong earthquake forces [9]. Historical buildings are an important part of the cultural heritage, due to their architectural value and construction techniques [10,11]. It is a responsibility to conserve these structures in order to pass them on to future generations [12,13]. The behavior of masonry buildings subjected to a moderate earthquake is poorly understood or investigated. The conservation of cultural heritage assets should ensure these buildings' capacity to survive against decay and natural hazards, without losing, as much as possible, their originality [12].

Historical buildings are an important part of the cultural heritage, due to their architectural value and construction techniques. It is a responsibility to conserve these structures to pass them on to future generations. The conservation of cultural heritage assets should ensure these buildings' capacity to survive against decay and natural hazards, without losing, as much as possible, their originality [12]. The behavior of masonry buildings subjected to a moderate earthquake is poorly understood or investigated [14]. Earthquakes are one of the main causes of damage to cultural heritage buildings across the world. Therefore, analyzing the seismic performance of cultural heritage assets is of great importance in order to determine effective structural improvement strategies [15]. Seismic performance analysis of historical structures is very complex and depends on many factors such as the geometry of the structure, mechanical properties of materials, connections between the walls, etc. [16]. Information about these variables can be obtained through measurements and laboratory tests [17].

Turkey is among the most seismically and tectonically active regions worldwide [18]. Over the past three decades, approximately twenty earthquakes with magnitudes exceeding M 6.0 have struck various parts of the country, resulting in the collapse or severe damage of numerous buildings [19]. Therefore, earthquake performance analysis of historical buildings in the country is an important and required step for the conservation of these buildings. The aim of this study is to analyze the material properties and seismic performance of a historical stone masonry cistern in Fethiye, Türkiye.

Some studies were performed on the seismic safety of historical buildings; Mutlu and Şahin [20] modeled the eastern minaret of the "Ulu Cami" in Bursa using the finite element method in the Sap2000 structural analysis software Ercan et al. [21] performed linear and nonlinear time history analyses of the updated finite element model of the minaret using the acceleration records of two different earthquakes that occurred in Türkiye. Usta and Bozdag [22] proposed a novel procedure for the immediate screening of masonry buildings at risk. This procedure is notable for its simplicity and speed, and it is based on a simplified geometric approach. Mustafaraj and Morina [23] conducted a structural assessment of Mehmed Pasha Hammam, a historical structure built during the 16th century in Prizren, Kosovo. Usta and Bozdag [24] utilised the finite element method (FEM) to assess the structural integrity of the Basdurak mosque. Asley and Okuyucu [25] examined Erzincan Değirmenliköy Church from a technical and structural perspective. Hysenlliu et al. [26] studied the effects of different materials on the seismic behavior of masonry buildings. Yurdakul et al. [27] determined the damages and locations of the damages that would occur in the case of different earthquakes in the historical Bayburt Ulu Mosque. Ahmadi et al. [28] proposed a new approach for estimating IDA curves using displacement-based adaptive propulsion (DAP) concepts. Structural behavior of the historic S. Giuseppe delle Scalze structure was analyzed by Ramaglia et al. [29] through the use of a FE model and various other models in predicting the major behavior of the structure. Seismotectonics of the area was studied by Doğangün et al. [30] which included the general behavior of earthquakes, along with the damages caused to the infill walls and the structure due to the seismic activities. Seismic behavior of the Totem Tower of Diar Es Saada, erected in 1953 in Algeria, was studied by Mohammedi et al. [31]. Demir et al. [32] conducted a study of the performance of buildings during the Sivrice-Elazığ earthquake, analysing the ground motion record time histories and response spectrum of that period. The study made a comparison between the practices of designing and construction with the Turkish Earthquake Code. Çelik and Tanriverdi [33] conducted a study on the repair and reinforcement options for vaults, with a particular focus on damage to joints and the upper parts of vaults. Ural and Çelik [34] conducted an analysis of the structural behaviour of the Tahtani (Stork) Mosque, employing the finite element method (FE) and the finite element analysis (FEA) to assess the effectiveness of tension rods between vault columns. Their analysis recommended the implementation of such rods to mitigate stress levels in the vaults, attributable to the mosque's substantial weight. In their 2021 study, Altunisik et al. conducted an analysis of the damage type and cause related to reinforced concrete and masonry structures during the Izmir-Samos earthquake. The study considered the conditions of the current Turkish Building Earthquake Design Regulation [35]. Fuzhang et al. [36] proposed a meshless methodology for obtaining solutions to three-dimensional multinomial time-dependent fractional partial differential equations (PDEs)). Pouraminian [37] utilised nonlinear methodologies in conjunction with finite element models to conduct a study on the seismic response of historical masonry buildings. Mohammed and Cesarano [38] examined the solutions to stochastic equations, offering both theoretical and practical explanations for their applications in physical and engineering contexts. Schiavoni et al. [39] conducted an investigation into the damage caused to the Santa Maria Annunziata church by the 2016 and 2017 Central Italy earthquakes. Sacco et al. [40] conducted a study on the structural damage to the historic San Carlo Borromeo church in Liguria, Italy, which has suffered due to a slow-moving landslide. The present study has sought to examine the effect of landslides on structures and to understand the associated damage and deformation mechanisms. This has been achieved by means of analysis, documentation, in situ observations, laser scanning and deformation studies. Sánchez et al. [41] developed a 3D finite element model and a 3D CAD model in OpenSees for the purpose of analysing the seismic performance of the historic Giralda tower in Seville, Spain. In order to achieve this objective, modal and nonlinear static analyses have been utilised. Sinai et al. [42] conducted an analysis of the structural behaviour and damage loads of Iranian brick masonry barrel vaults, focusing on the impact of skew angle. An experimental approach was adopted to assess the properties of materials and the performance of vaults under gravity loads. A finite element model has been created and analysed numerically. The numerical and experimental results have been compared based on the Willam-Warnke fracture criterion. The study performed by Sokhtesaraei et al. [43] focused on selection of two-component pairs of accelerograms out of 1000 pairs recorded during Iranian earthquakes occurring in 1978-2010 to serve as appropriate acceleration histories of ground motion for further analysis and assessment of the structure in Tehran. Aykanat et al. [44] carried out a field study to record the damages and collapses caused during the earthquake of 23 November 2022 at 04:08 LT in the Gölyaka district of Düzce Province, Turkey (Western Black Sea Region). Güner and Nuhoğlu [45] have introduced a new lattice-model-based method for characterising the in-plane behaviour of walls. The main parameters of this model are: the slope, the cross section area, the mesh size, and the material characteristics. Altunisik et al. [46] gave a detailed review of the most common structural weaknesses in reinforced concrete buildings situated in urban seismic areas. Special attention should be paid to the earthquake in Kahramanmaraş of 6 February 2023. In their paper, Sevim et al. [47] applied documentary and visual materials for studying the damages of affected buildings due to the double earthquake event in Kahramanmaraş. The earthquakes took place on 6 February 2023 at 04:17 LT in the Pazarcık district (Mw 7.7) and roughly nine hours later in the Elbistan district (Mw not specified). Hacıefendioğlu et al. [48] presented an automated damage assessment technique for masonry buildings after an earthquake using deep learning segmentation approach in which U-net CNN model is employed.

Structural Description of the Historical Cistern

The cistern structure is located in Esenkoy, Fethiye. It was built in the 1800s during Ottoman Period. The floor area of the building has a rectangular shape and the structure has a vaulted roof. The short side length of the structure is 8.43 m. and the long side length and also the length of the vault is 13.5 m. Figure 1 shows the location of the cistern structure and seismic map of Turkey.

The walls of the historical cistern, made from rubble, carved stones, and mortar, form a composite element for practical analysis, treated as a single entity in macro model analysis (Yurdakul et al. [27]). The behavior of the walls made out of masonry depends on the properties of the material used for building, which are masonry and mortar. The behavior of masonry walls can differ drastically because of the material properties and the way the structure was built. The parameters such as craftsmanship, joint size, and wall dimensions are important, and the use of improper material affects greatly the behavior of the walls [49].

In order to analyze historical buildings by using the finite element method (FEM) correctly, the mechanical properties of the materials of the building should be examined experimentally. This study aimed to determine the mechanical properties of the stone used in the construction of the historical cistern. The specimens were obtained from the actual structure. Eight different samples were tested following the TS EN 1926 Turkish standard (Natural stone test methods - Determination of uniaxial compressive strength) [50] for measuring compressive strength. This standard covers a method for maintaining the uniaxial compressive strength of natural stone. The methodology involved the application of a monotonically increasing axial load (4.71 MPa/s) until failure. The test scheme is presented in Figure 2. Such testing procedure was very useful for determining the properties of the stone.

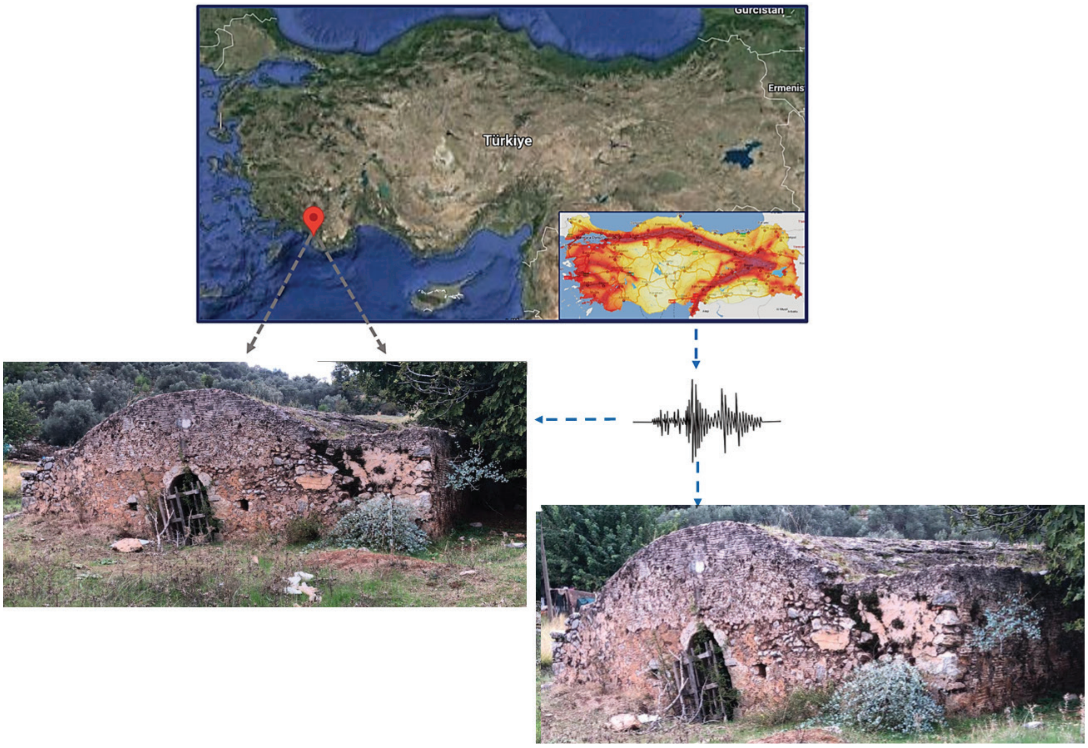

Figure 1. The seismic map of Türkiye and the location of the cistern structure.

Figure 2. The experimental setup for the determination of mechanical properties.

Eight 50 mm cube specimens were tested under compression using a 500 kN capacity hydraulic testing machine. The compressive strength was calculated by dividing the peak load recorded during testing by the specimen's cross-sectional area. [51]. Experimental results are presented in Table 1. The stone's average compressive strength was calculated as 62.56477 MPa. The average compressive strength of the stones was determined as 62.56 MPa based on experimental results. This value aligns with the range of compressive strengths obtained for similar stone structures by Senthivel and Lourenço [8]. Additionally, Çoban [52] highlighted in his study that the strength of stone and mortar composite elements corresponds to approximately 70% of the stone strength.

Static modulus of elasticity of masonry stones defined by many standards can be calculated empirically. Eq. (1) can be used to determine the modulus of elasticity depending on compressive strength [53].

$$E_{mas} = 750.f_{c,mas} \quad (1)$$

Where $f_{c,mas}$ (N/mm^2) is the characteristic compressive strength of the stone and E_{mas} (N/mm^2) is the modulus of elasticity of the stone.

In historical masonry structures, stone and mortar act together as a composite material. For practical numerical analyses, this composite masonry is commonly represented as a single equivalent material, which is referred to in the literature as the macro-modelling approach [54]. In the present study, since the mechanical properties of the stone–mortar composite could not be directly determined, the masonry units and mortar were modeled together as a homogenized material. Based on the literature [52], the mechanical properties of this equivalent composite material were assumed to be 70% of the corresponding values of the stones or bricks.

Table 1. The experimental results of cistern stones

Sample No	Area (mm^2)	Density (kg/cm^3)	Load speed (kN/s)	Maximum Load (kN)	Compressive Strength (MPa)
1	2500	3.28	4.71	185.68	74.27
2	2500	2.71	4.71	169.98	67.99
3	2500	2.91	4.71	180.70	72.28
4	2500	2.71	4.71	48.17	19.27
5	2500	2.40	4.71	141.90	56.76
6	2500	2.74	4.71	211.42	84.57
7	2500	2.94	4.71	149.52	59.81
8	2500	2.80	4.71	163.94	65.58
Avg. values		2.81		156.41	62,56

3D Finite Element Model of the Cistern

The cistern described in this study is an 18th-century water storage structure, primarily designed to provide a storage area insulated from external factors to prevent water deterioration. Therefore, only the main entrance opening was considered in both the actual design and the modeling of the structure. Small openings in the walls were not included in the model because such openings are not present in the structure. This modeling approach aligns with general architectural characteristics and historical usage of cistern structures. The model of the cistern was developed using the SAP2000 V22 finite element program [55]. The masonry walls were discretized using 10,595 three-dimensional, eight-node, six-sided solid elements and 15,088 nodes. The maximum and minimum dimensions of the solid elements were approximately 0.2 m × 0.2 m × 0.1 m and 0.1 m × 0.1 m × 0.2 m, respectively.

In the SAP2000 finite element model, S33 represents the axial tensile and compressive stresses in the Z direction, while S11 and S22 correspond to the axial tensile and compressive stresses in the other principal directions. These stress components were considered during the analysis and evaluation stages of the study, as shown in Figure 3.

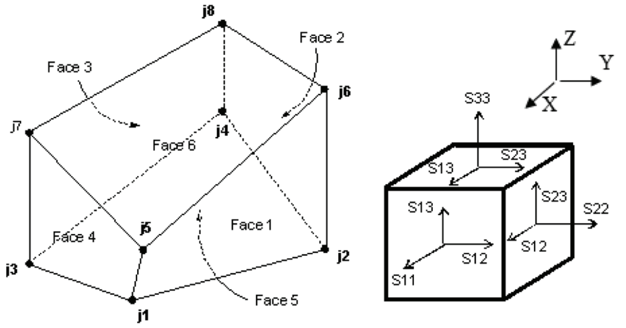

a) 8- node solid element b) Stress components in the global coordinate

Figure 3. A solid element

The base of the cistern was considered to be fixed. The roof was considered a structural component in the model. The FEM model has a total mass of 1098.22 metric tons. Geometrical second-order effects were neglected in the analyses. Modal analysis was performed using the eigenvector method in SAP2000. In accordance with the macro-modelling approach, the masonry structure was assumed

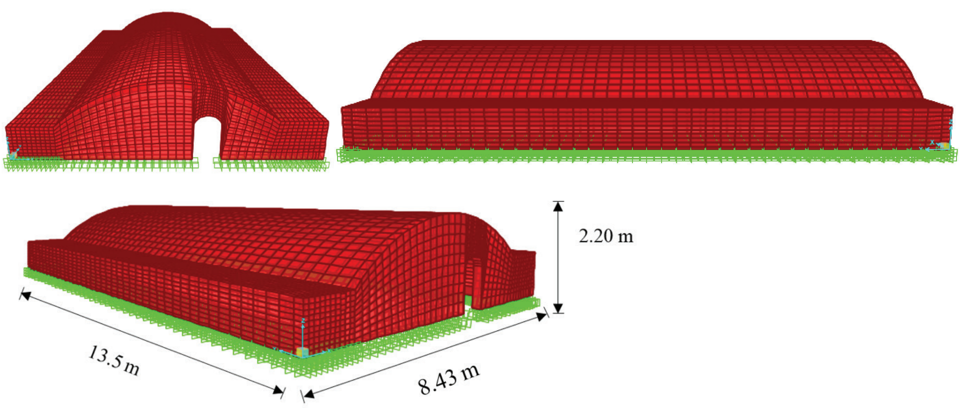

Figure 4. FEM model of the cistern.

to behave as a homogeneous material. In this study, macro-modelling was adopted because it is more appropriate for the dynamic analysis of complex, large-scale historical structures [27]. The finite element model of the cistern is presented in Figure 4.

Strong Motion Selection

To select hazard-compatible ground motions for linear dynamic analysis of the structural model, we chose Strike-Slip ground motions from the PEER database [56,57]. During the selection of ground motion records, 30records were identified using the PEER (Pacific Earthquake Engineering Research) database. These records focused on far-field earthquakes with a strike-slip mechanism, magnitudes ranging from 6.5 ≤ M ≤ 7.5, and shear wave velocities (Vs30) between 360 and 760 m/s. These criteria were chosen to ensure compatibility with the seismic hazard profile of the study region. The chosen earthquake records were scaled to match the DD2 earthquake design levels as per the Turkish Earthquake Hazard Map. During the entire scaling phase, each earthquake record was made consistent with the elastic design spectrum. More specifically, the values of spectral acceleration (Sa(T1)) were modified to match the targeted spectrum for the fundamental period of the structure, and the scaling factor was established. It has been found that this technique increases the accuracy of the records and analyses. Moreover, different parameters, such as PGA, PGV, and Arias Intensity, have been used in each analysis process. These parameters helped in conducting a more extensive analysis of the impact of ground motion on the seismic demands. The records have been presented in Table 2 and Figure 5.

Table 2. Set of 30 ground motion records from strike-slip mechanism

Earthquake Name	Year	Magnitude	Mechanism	Rjb (km)	Rrup (km)	Vs30 (m/sec)
"Parkfield"	1966	6.19	strike slip	17.64	17.64	408.93
"Northern Calif-05"	1967	5.6	strike slip	27.36	28.73	219.31
"San Fernando"	1971	6.61	Reverse	19.33	22.63	450.28
"Coyote Lake"	1979	5.74	strike slip	19.46	19.7	335.5
"Imperial Valley-06"	1979	6.53	strike slip	22.03	22.03	242.05
"Imperial Valley-06"	1979	6.53	strike slip	17.94	17.94	196.88
"Irpinia_ Italy-02"	1980	6.2	Normal	22.68	22.69	574.88
"Taiwan SMART1(5)"	1981	5.9	Reverse	26.31	27.36	268.37
"Morgan Hill"	1984	6.19	strike slip	13.68	13.69	270.84
"N. Palm Springs"	1986	6.06	Reverse Oblique	10.08	10.84	312.47
"Chalfant Valley-01"	1986	5.77	strike slip	14.99	15.13	585.12
"Whittier Narrows-01"	1987	5.99	Reverse Oblique	13.58	20.91	346.62
"Superstition Hills-02"	1987	6.54	strike slip	18.2	18.2	192.05
"Loma Prieta"	1989	6.93	Reverse Oblique	24.27	24.57	239.69
"Landers"	1992	7.28	strike slip	26.96	26.96	355.42
"Northridge-01"	1994	6.69	Reverse	23.5	29.88	297.07
"Kobe_ Japan"	1995	6.9	strike slip	24.85	24.85	256
"Manjil_ Iran"	1990	7.37	strike slip	12.55	12.55	723.95
"Chi-Chi_ Taiwan-04"	1999	6.2	strike slip	21.62	21.67	258.89
"Cape Mendocino"	1992	7.01	Reverse	23.46	25.91	515.65
"Tottori_ Japan"	2000	6.61	strike slip	28.81	28.82	293.37
"Parkfield-02_ CA"	2004	6	strike slip	12.59	12.97	357.35
"Niigata_ Japan"	2004	6.63	Reverse	17.57	18.03	193.2
"Chuetsu-oki_ Japan"	2007	6.8	Reverse	15.89	23.44	430.16
"Iwate_ Japan"	2008	6.9	Reverse	20.47	20.64	264.48
"Iwate_ Japan"	2008	6.9	Reverse	10.71	13.47	361.24
"El Mayor-Cucapah_ Mexico"	2010	7.2	strike slip	13.21	15.91	242.05
"Joshua Tree_ CA "	1992	6.1	strike slip	21.73	22.3	396.41
"Darfield_ New Zealand"	2010	7	strike slip	24.36	24.47	422
"Christchurch_ New Zealand"	2011	6.2	Reverse Oblique	16.6	16.61	249.28

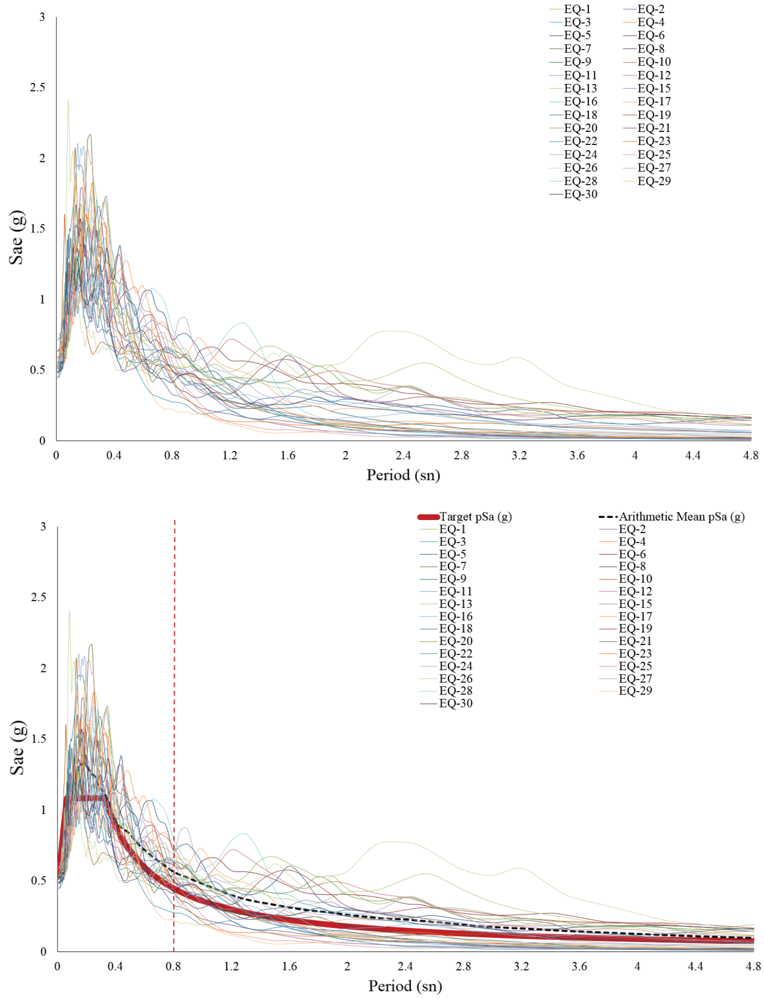

Figure 5. a) Response spectra set of 30 records from different source mechanisms to be used in THA analysis. Unscaled signals: (b) Response spectra set of records scaled to spectral acceleration at the structural period in the X direction, Sa (T1, 5%).

Unscaled signals: (b) Response spectra set of records scaled to spectral acceleration at the structural period in the X direction, Sa (T1, 5%).

Wall Characteristic Shear Strength

The characteristic shear strength of masonry walls can be calculated with the help of Equation (2) as specified in TBDY-2018 [53].

$$f_{vk} = f_{vko} + 0.4\,\sigma \leq 0.10\,f_b \qquad (2)$$

In this equation;

f_{vk}: Characteristic shear strength of masonry wall,

f_{vko}, the characteristic initial shear strength

σ: Earthquake loads multiplied by load coefficients and vertical compressive stress calculated under the influence of vertical loads,

f_b: It is the average compressive strength of the masonry unit.

To calculate the shear stresses on the cistern walls and their shear strength, we followed the nomenclature shown in Figure 6.

RESULTS AND DISCUSSION

The Cistern was modeled with solid elements. The modes of vibration and the values of participation of the modal responses were determined by a discretization in finite elements by SAP2000 Software. Model Periods and modal participating mass ratios are shown in Table 3.

The linear elastic time history analysis of the cistern structure was performed in this paper. The modal mass participation ratios were found to exceed 93% in the analyzes conducted with the SAP2000 software. Pardalopoulos and Pantazopoulou [58] highlight the importance of high mass participation ratios in modal analyses for the accurate modeling of the dynamic characteristics of the structure.

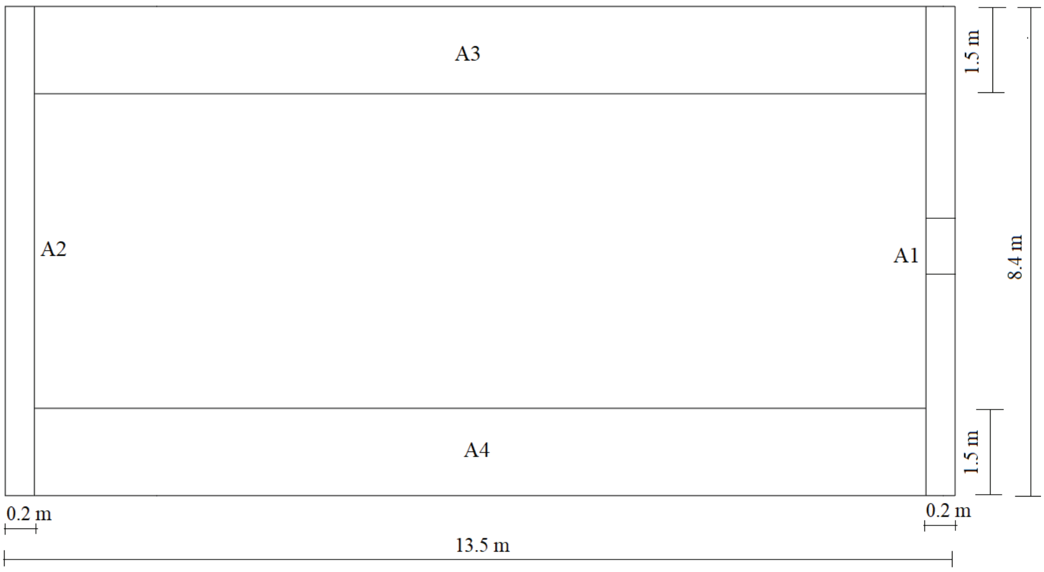

Figure 6. Plan view of the cistern.

Table 3. Model periods and modal participating mass ratios

StepNum Unitless	Period Sec	Frequency Cyc/sec	UX Unitless	UY Unitless	UY Unitless
1	0.025	30.901	0.066	5.52E-08	4.81E-05
2	0.018	56.855	3.31E-07	2.54E-07	1.13E-07
3	0.013	77.982	0.006635	4.5E-07	4.43E-06

Accordingly, the ratios obtained in the study are in accordance with the findings of previous studies.

As shown in Figure 2, the eigenvalue analysis of the finite element model produced numerous closely spaced vibration modes. The first few modes were generally associated with negligible modal mass and were therefore of limited relevance. Consequently, a large number of modes had to be included in each principal plan direction of the

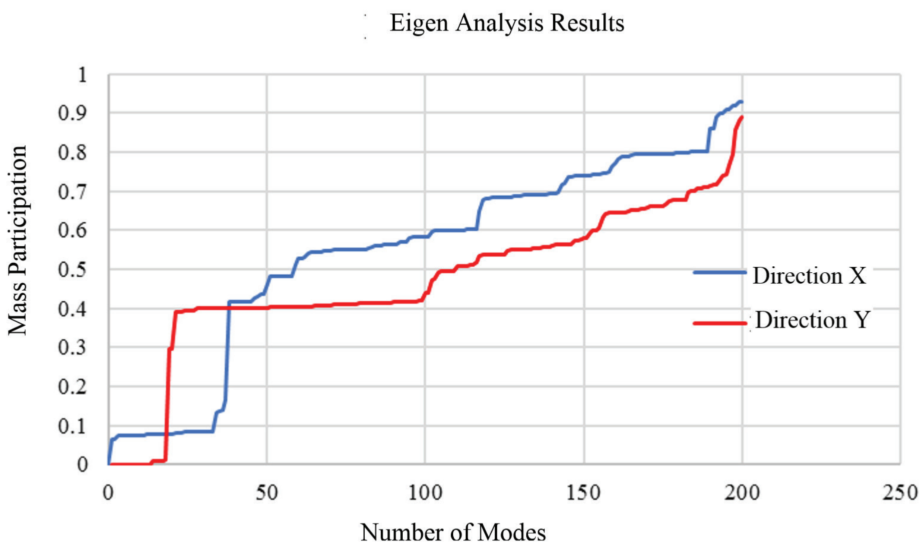

Figure 7. Percentage of total mass participation in the X and Y plan directions after considering the first 200 modes.

Figure 8. The periods and participation factors of the 200 modes.

structure to achieve an adequate level of total mass participation [58]. The periods and modal participation mass ratios (MPMRs) of the first 200 modes are presented in Figure 7 and 8.

The selection of the number of modes for the cistern structure in the study was based on achieving sufficient dynamic mass participation to ensure accurate seismic behavior representation. During the modal analysis carried out using SAP2000, there were a total of 200 modes included, and this has led to a mass participation ratio being in excess of 93% in both principal directions. The mass participation ratio being high means that a major portion of the dynamic properties of the structure has been taken into consideration, and therefore the need to consider higher modes is eliminated. In the case of the cistern structure, which is a one-story, high occupancy masonry structure with rigid walls and no intermediate stories, the effect of higher modes in the response of the entire structure will be very small. Such structures have a tendency of having modal participation from lower modes due to the properties of the structure. If further confirmation is needed, a sensitivity analysis incorporating even higher modes could be conducted, but based on the study results, the current approach aligns well with the structural properties and intended performance evaluation of the cistern.

Features such as duration, Pga, and acceleration values of Ground motion records caused each earthquake record to give different results on the structure. The maximum displacement values obtained from the earthquake records used in the article and vary depending on the characteristics of the earthquakes are given in Table 4.

The horizontal displacement values presented in the table range from 0.070 cm to 1.500 cm in the X direction and from 0.034 cm to 0.288 cm in the Y direction. When compared with the critical thresholds specified in the literature, these values provide important information about the seismic performance of the structure. Vicente et al. [12] noted that horizontal displacement values exceeding 0.5 cm in masonry structures accelerate crack formation and lead to significant stress concentrations. In this context, high displacement values such as Joshua Tree (1.500 cm in the X direction, 0.288 cm in the Y direction) and Parkfield-02_CA (1.124 cm in the X direction, 0.147 cm in the Y direction) indicate a serious potential for damage around the dome openings and entrance areas.

Lagomarsino and Cattari [59] emphasized that horizontal displacement values exceeding 1.0 cm could cause crack intensification in rigid regions. In the table, Loma Prieta (1.336 cm in the X direction) exceeds this threshold and poses a risk of crack formation in the openings. On the other hand, lower displacement values (e.g., San Fernando: 0.175 cm in the X direction, 0.049 cm in the Y direction) indicate a lower risk of damage in the rigid regions of the structure.

Hysenlliu et al. [26] stated that maximum displacement values exceeding 0.3 cm in masonry structures with different materials could lead to the onset of crack formation in weak areas. According to the table, displacement values measured in the Y direction, such as Joshua Tree (0.288 cm) and Iwate_Japan (0.071 cm), are close to or above this threshold and may pose a risk of damage in weak areas.

Studies in the literature suggest that interstory drifts can be used to determine structural damage [60-62]. According to the studies, the suggested performance limit states corresponding to the local failure modes of inter-story drift ratios are given in Table 5.

The drift ratio used in the study, which is commonly employed as a criterion for structural performance evaluation, was utilized to determine the performance levels in our work. The limit values of drift ratios were based on the references of [64,65].

Table 4. Properties of earthquake records and time history results

No	Earthquake Name	Pga (g)	Pgv (cm/sn)	Arias Intensity (m/sec)	Scale Factor	Max Displacement (cm)	
						X Direction	Y Direction
EQ-1	"Parkfield"	0.06	7.20	0.1	6.06	0.205	0.172
EQ-2	"Northern Calif-05"	0.18	11.52	0.1	2.28	0.660	0.076
EQ-3	"San Fernando"	0.29	22.18	1	1.27	0.175	0.049
EQ-4	"Coyote Lake"	0.10	6.86	0.1	3.60	0.222	0.118
EQ-5	"Imperial Valley-06"	0.26	26.95	3.3	1.13	0.658	0.059
EQ-6	"Imperial Valley-06"	0.14	22.27	0.4	2.59	0.980	0.046
EQ-7	"Irpinia_ Italy-02"	0.14	11.40	0.3	3.24	0.174	0.105
EQ-8	"Taiwan SMART1(5)"	0.17	9.04	0.2	2.61	0.160	0.101
EQ-9	"Morgan Hill"	0.17	12.33	0.2	2.37	0.846	0.083
EQ-10	"N. Palm Springs"	0.07	6.53	0.3	2.03	0.070	0.047
EQ-11	"Chalfant Valley-01"	0.07	5.66	0	5.28	0.997	0.058
EQ-12	"Whittier Narrows-01"	0.26	43.67	0.1	4.41	0.906	0.208
EQ-13	"Superstition Hills-02"	0.16	25.55	1.1	1.26	0.528	0.034
EQ-14	"Loma Prieta"	0.21	37.87	0.5	2.19	1.336	0.139
EQ-15	"Landers"	0.12	12.49	0.4	2.83	0.787	0.049
EQ-16	"Northridge-01"	0.19	16.59	0.7	1.73	0.217	0.053
EQ-17	"Kobe_ Japan"	0.21	21.15	0.6	1.84	0.278	0.050
EQ-18	"Manjil_ Iran"	0.52	49.48	7.5	0.62	0.251	0.056
EQ-19	"Chi-Chi_ Taiwan-04"	0.17	18.85	0.4	2.10	0.183	0.047
EQ-20	"Cape Mendocino"	0.25	34.21	0.9	1.42	0.258	0.067
EQ-21	"Tottori_ Japan"	0.31	16.27	0.8	1.31	0.310	0.066
EQ-22	"Parkfield-02_ CA"	0.20	6.88	0.1	2.79	1.124	0.147
EQ-23	"Niigata_ Japan"	0.34	20.41	0.8	1.19	0.282	0.047
EQ-24	"Chuetsu-oki_ Japan"	0.11	8.84	1.8	1.20	0.767	0.048
EQ-25	"Iwate_ Japan"	0.26	12.75	1.9	1.38	0.201	0.071
EQ-26	"Iwate_ Japan"	0.44	59.06	4.2	0.85	0.315	0.069
EQ-27	"El Mayor-Cucapah_Mexico"	0.43	54.92	6.1	0.72	1.041	0.090
EQ-28	"Joshua Tree_ CA "	0.10	9.10	0.2	3.66	1.500	0.288
EQ-29	"Darfield_ New Zealand"	0.57	31.85	4.1	0.69	0.286	0.080
EQ-30	"Christchurch_ New Zealand"	0.11	11.78	0.2	2.99	1.105	0.094

Table 5. Performance levels in terms of drift ratios based on local failure modes (adapted from Demirel [63])

		Performance Level (Drift Ratio)		
Author	Failure Mode	IO	LS	CP
Franklin et al. (2001) [64]		0.1	0.9-1.5	1.2-1.9
Bosiljkov et al. (2008) [65]		0.1	1.2-1.8	1.8-2.5
Bosiljkov et al. (2008) [65]	Sliding	-	0.9	1.8
Bosiljkov et al. (2008) [65]	Diagonal Tension	0.2-0.5	0.5-0.7	0.5-0.9
Alcocer et al. (2004) [66]		0.15	0.25	0.4

The drift ratios of the cistern walls obtained from linear dynamic Time History Analyses were presented in Table 6.

Cistern structure exhibits a very rigid behavior since it is a single storey and void-free structure with a very high occupancy rate. For this reason, the drift ratio ratios in the building are at low values as seen in the table. The measured drift ratios of the Cistern Facade walls are between 0.0004 - 0.008 in the short direction and 0.0016- 0.0002 in the long direction Since these drift ratio values do not exceed the 0.1 limit value, which represents the Immediate Occupancy

Table 6. Drift ratios of the cistern

Earthquake Name	Drift Ratio (X direction)	Performance Level	Drift Ratio (Y direction)	Performance Level
EQ-1	0.0011	IO	0.0010	IO
EQ-2	0.0037	IO	0.0016	IO
EQ-3	0.0010	IO	0.0012	IO
EQ-4	0.0012	IO	0.0008	IO
EQ-5	0.0037	IO	0.0008	IO
EQ-6	0.0054	IO	0.0007	IO
EQ-7	0.0010	IO	0.0006	IO
EQ-8	0.0009	IO	0.0006	IO
EQ-9	0.0047	IO	0.0005	IO
EQ-10	0.0004	IO	0.0005	IO
EQ-11	0.0055	IO	0.0005	IO
EQ-12	0.0050	IO	0.0004	IO
EQ-13	0.0029	IO	0.0004	IO
EQ-14	0.0074	IO	0.0004	IO
EQ-15	0.0044	IO	0.0004	IO
EQ-16	0.0012	IO	0.0004	IO
EQ-17	0.0015	IO	0.0004	IO
EQ-18	0.0014	IO	0.0003	IO
EQ-19	0.0010	IO	0.0003	IO
EQ-20	0.0014	IO	0.0003	IO
EQ-21	0.0017	IO	0.0003	IO
EQ-22	0.0062	IO	0.0003	IO
EQ-23	0.0016	IO	0.0003	IO
EQ-24	0.0043	IO	0.0003	IO
EQ-25	0.0011	IO	0.0003	IO
EQ-26	0.0018	IO	0.0003	IO
EQ-27	0.0058	IO	0.0003	IO
EQ-28	0.0083	IO	0.0003	IO
EQ-29	0.0016	IO	0.0003	IO
EQ-30	0.0061	IO	0.0002	IO

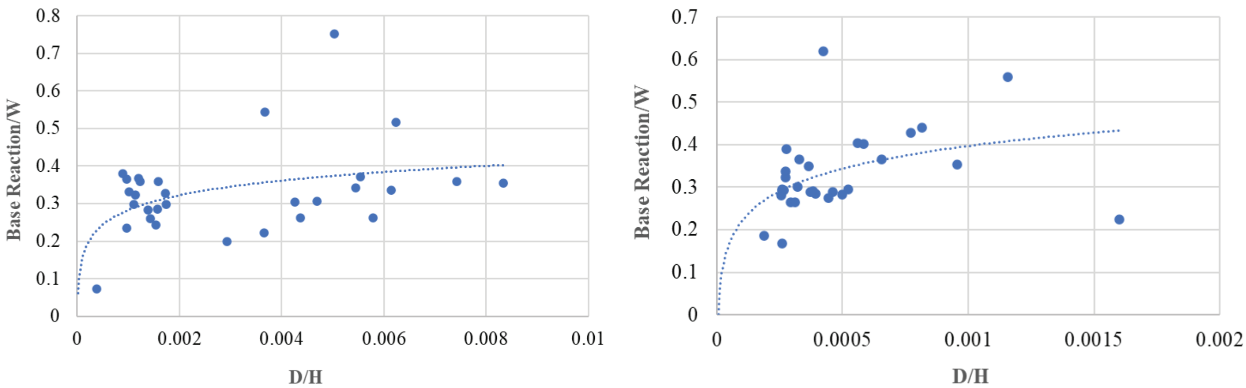

Figure 9. Pushover curves X and Y directions FE model of Cistern Structure.

performance level, the structure is expected to show slight damage during the described earthquakes and earthquakes similar to these earthquakes. In addition, when looking at the building directions, it was seen that the displacement values in the X direction (short direction) of the building were larger than the Y direction (longer direction). This is an indication that the long side of the building is more rigid than the short side.

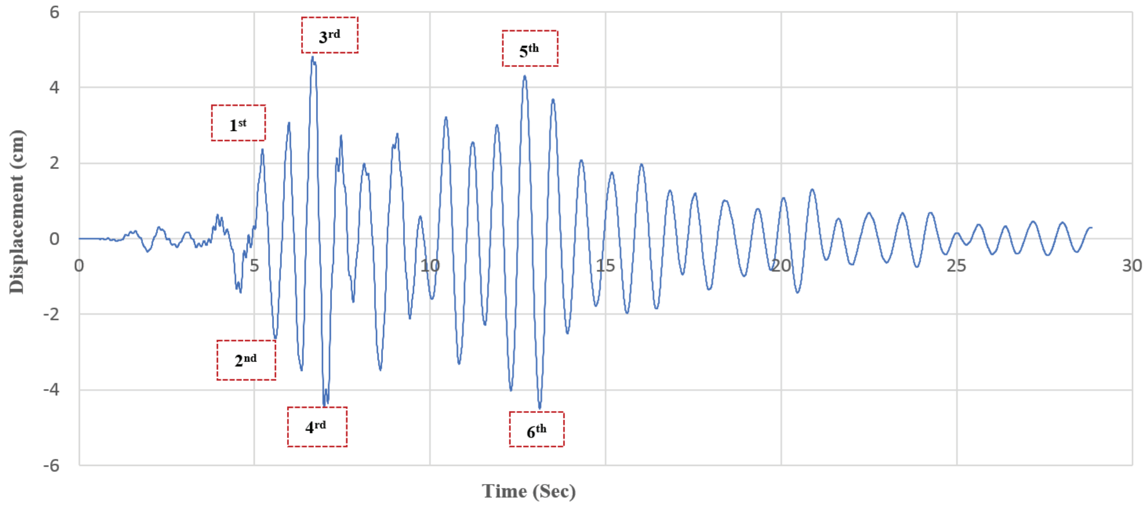

Figure 10. The displacement - time graph for EQ28.

The pushover curves, expressed as generalized force–displacement relationships, are presented in Figure 9 for loading applied in the ±X direction (North–South) and ±Y direction (East–West). To obtain the capacity curves, the control node was selected as the node located at the top of the cistern that exhibited the maximum horizontal displacement.

In practical assessment methodologies, it is commonly observed that finite element models of masonry monuments subjected to real earthquake time histories may predict severe damage, whereas the actual structures often exhibit lower levels of damage. During seismic loading, cracks progressively open from small to larger widths at peak loading cycles, which increases the structure's capacity to absorb seismic energy [67]. In order to better see and interpret the responses of earthquakes in the structure, the earthquake named EQ28, which is one of the earthquakes that give the highest displacement values in the structure was chosen.

The displacement - time graph for the earthquake is presented in Figure 10.

For the relevant parts of the displacement time graph of the earthquake, the response of the structure at certain time instants and the stress graphs are shown in Figure 11.

These stresses are considered critical in terms of crack formation and propagation. Specifically, tensile stresses around the door and dome openings are identified as the primary causes of structural damage during seismic impacts.

According to the data presented in Figure 11, compressive and tensile stresses are particularly concentrated around the dome openings and entrance walls. In terms of compressive stresses**,** the highest values were observed around the dome openings and the surrounding area

EQ28X (MPA)

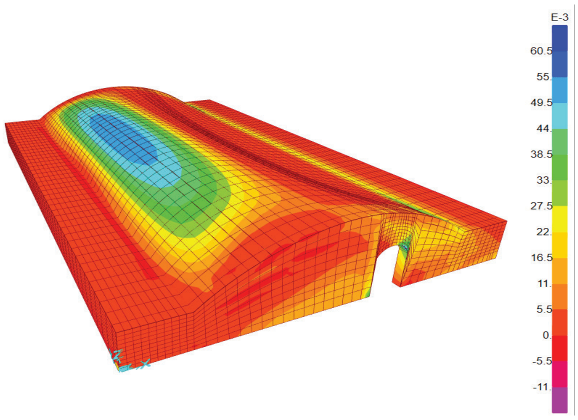

EQ28Y (MPA)

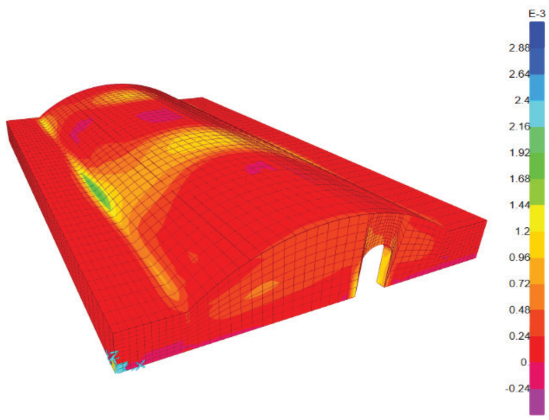

T: 5.25 sn

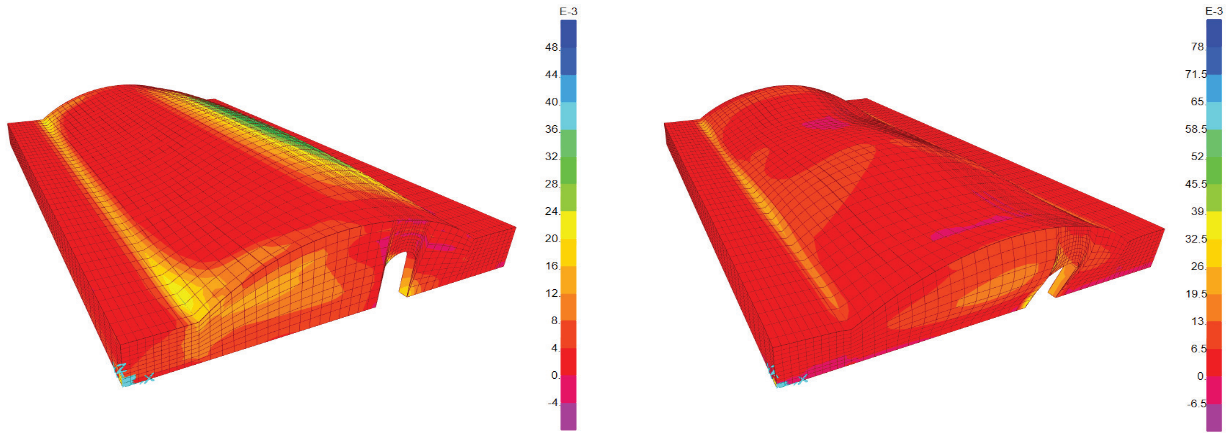

T: 5.60 sn

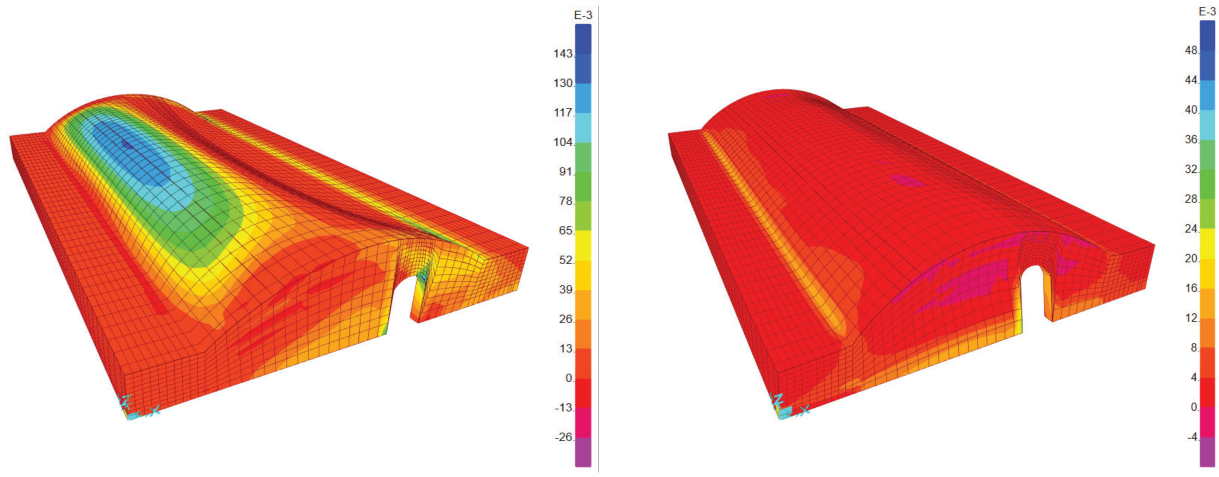

T: 6.63 sn

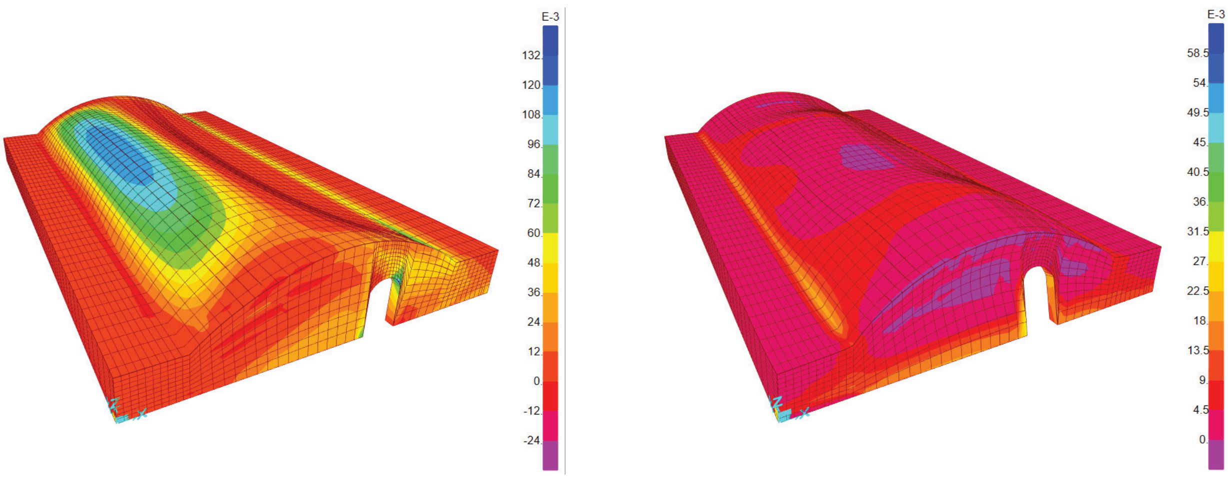

T: 7.09 sn

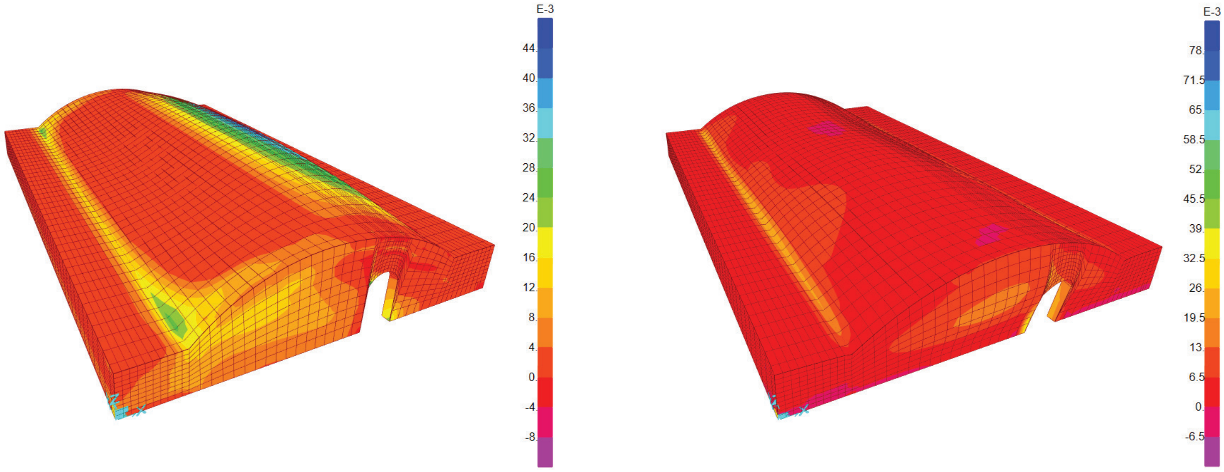

T: 12.75 sn

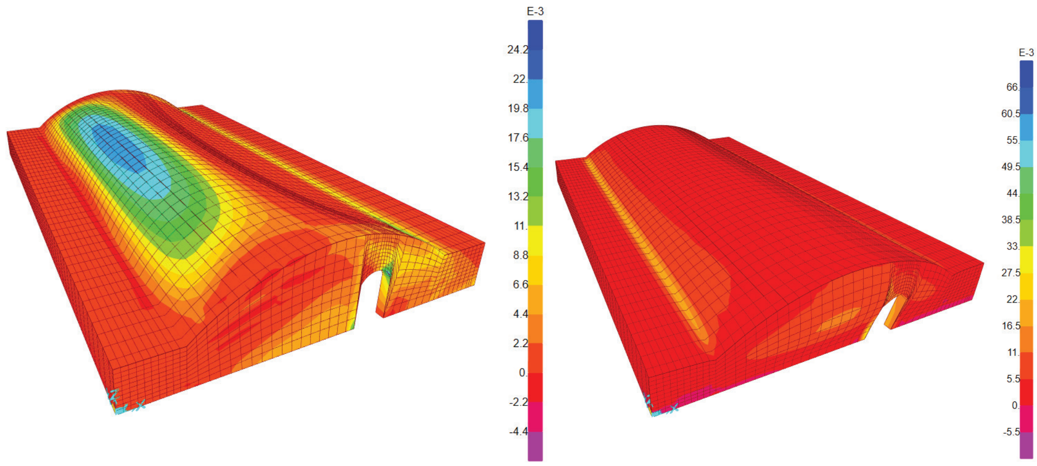

T: 13.13 sn

Figure 11. Distribution of stresses and deflection in the structure using time history analysis for the earthquake named EQ28

of the entrance wall. The maximum compressive stress was approximately 0.525 MPa, indicating critical zones of localized stress accumulation identified in the model. These areas underscore the necessity for structural reinforcement. Conversely, tensile stresses were predominantly concentrated in the dome apertures and the upper section of the entrance door. The analysis presented in Figure 11 revealed that the maximum tensile stress was calculated to be approximately 0.272 MPa.

These findings are crucial for understanding the current stress distribution within the cistern structure and for identifying priority intervention areas.

From these graphs, the damage (cracking and stress) values n the walls can be seen and the damage in the structure can be defined qualitatively.

During an earthquake, as cracks occur in the walls and the structure is damaged, the strength of the structure decreases.

While the cistern structure is displaced in the same direction, the crack tip continues to propagate, while stress relaxation is observed in the previously cracked parts. When the structure starts to move in the opposite direction, the cracks can close and compressive stresses can be seen in the already cracked places.

Crack propagation and stress concentration were observed, particularly around the dome and wall openings. The structure maintained its structural integrity under most earthquake scenarios [59] stated that similar stress and damage mechanisms could occur in stone structures with large openings under seismic effects. This demonstrates the consistency of the findings with the literature.

In some cases, early damage caused by high seismic intensity may lead to a reduced acceleration response of the structure during subsequent stronger phases of the record. This behavior may be attributed to damage-induced elongation of the structural vibration period, which can reduce the acceleration demand and allow the structure to survive the earthquake. Therefore, in such situations, the observed response is governed not only by the intensity of the acceleration but also by the sequence, timing, and damage progression during the ground motion [58].

A comparison between the numerical results obtained from the seismic analysis and the observed damage patterns on the historical cistern structure provides critical insights into the accuracy of the model and the seismic behaviour of the structure. In the subsequent analysis section, the observed level of damage was subjected to a comparative analysis with the actual damages sustained. Based on the numerical analysis, stress concentrations become evident mostly around the primary dome and wall holes. It is worth noting that the findings are consistent with the field observation, as damage is evident mostly in these parts. However, according to the numerical analysis, there is a slightly higher level of stress at the center of the dome compared to the stress that causes the minor cracks. The difference can be attributed to the actual properties of the material or method of construction used in real life. The findings further suggest possible ways through which damage occurs, for instance, due to high shear stress near the door holes. This is thoroughly illustrated in Figure 12.

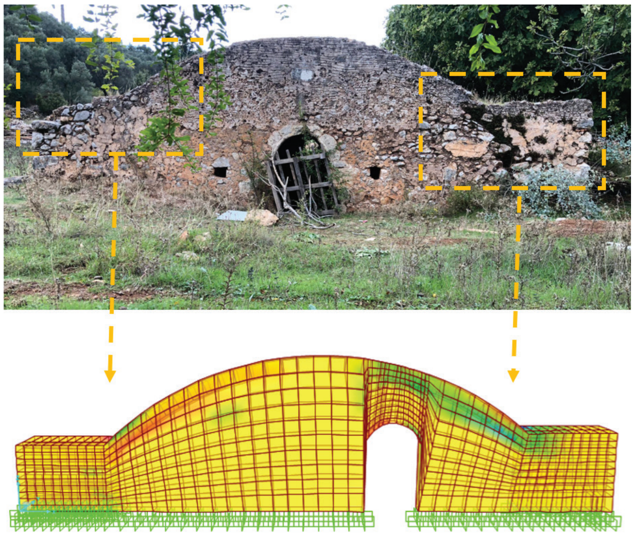

Figure 12. Stones detached from the vertical wall due to shear stresses.

The characteristic shear strength of the wall is calculated with the help of Equation (2). In this equation, f_{vko}, the characteristic initial shear strength is given as 0.1 MPa for natural or artificial stones in TBDY 2018 [53]. The characteristic shear strengths calculated for the walls and the shear stresses occurring in these walls are shown in Table 7.

While obtaining Table 7, the characteristic shear strength was calculated for each wall and these strengths were compared with the greatest shear stresses resulting from time history analyses. According to time history analysis, the largest shear stresses occurred as a result of the EQ28 earthquake. For this reason, only the shear stresses obtained for the x and y components of the EQ28 earthquake are shown in Table 7.

Shear strength and stress values determined from the analysis of the cistern walls as provided in Table 7 reveal uniform agreement with similar research in the literature. The maximum value of shear stress in this research, for instance, 0.272 MPa for wall A1 in Y direction, agrees with the shear stress concentration in masonry walls with openings as reported by Kumbasaroglu et al. [16]. The increased values of shear stresses around door openings confirm the existing literature where the same areas have been noted as weak points in the structure. Hrasnica and Medic [9] have pointed out that stone masonry structures generally suffer from weaknesses in the shear strength in the vicinity of openings, which calls for immediate attention to strengthen those structures through retrofitting works. The results obtained in this research indicating that wall A1 lacks

Table 7. Shear strengths and shear stresses for the walls

Direction	Wall	Compressive stress, σ (MPa)	Characteristic shear strength, fvk (MPa)	The maximum shear stress that occurs (MPa)
X	A1	0.218	0.187	0.147
	A2	0.226	0.190	0.092
	A3	0.525	0.310	0.059
	A4	0.512	0.305	0.064
Y	A1	0.218	0.187	0.272
	A2	0.226	0.190	0.023
	A3	0.525	0.310	0.079
	A4	0.512	0.305	0.080

adequate shear strength are in line with this observation. However, the shear stresses in X direction of all walls were less than their respective shear strengths. Such a conclusion corresponds to the results of the work of Senthivel and Lourenço [8], which stated that masonry structures usually demonstrate higher strength in the X direction. As can be seen from the results obtained, they mostly correspond to existing literature and validate the efficiency of using modelling and experimental validation for assessment of the behaviour of masonry structures in relation to the effects of the seismic load. The found weakness of the Wall A1 and accordance with literature data concerning the influence of openings show the necessity of the use of the proposed techniques for retrofitting. In this case, high-strength mortar injection and use of horizontal steel rods as proposed by Çelik and Tanriverdi [10] are highly effective techniques for reducing the shear stress.

After performing the static analysis, the vertical load of the wall was equal to 6159.663 kN. Vertical compressive stress of the wall at such a load was 0.171 MPa.When these values are used, the characteristic shear strength f_{vk} according to Equation (1) is obtained as 0.168 MPa. When Figure 11 is examined, the largest shear stress in the cistern as a result of earthquake ground movements is 0.136 MPa. This result shows that the cistern is safe in terms of shear stress.

There are cracks due to the building's aging and depreciation over time. Plaster shedding also was observed in some areas. In these parts, where masonry units are missing, the growth of vegetation can be easily seen from field observations and Figure 11. Furthermore, Considering the analysis results, it was seen that the greatest shear stresses occurred in the wall area on the right side of the building entrance. In the current state of the building, this area is already damaged. The damaged area on the current structure is less wide in relation to the corresponding area on the model. The compatibility of the analysis result with the current situation shows the accuracy of the modeling and analysis.

CONCLUSION

Historic cisterns are important components of cultural heritage due to their architecture and function. Nevertheless, little has been researched about their unique architectural forms and susceptibility to earthquakes. Most studies are dedicated to common masonry structures and do not consider the specificities of cisterns, including their roofs, openings, and underground parts. Lack of relevant information has made it difficult to develop effective measures of strengthening historic cisterns to ensure their seismic resistance. This paper discusses the seismic performance of the historic cistern in Fethiye, Turkey. Experimental and numerical methods were used to conduct an in-depth analysis of the cistern and obtain important findings. The mechanical properties of stone materials were defined; earthquake accelerations were set according to the Turkish Building Earthquake Code (2018). Static and time-history analyses of the cistern were conducted with SAP2000 V22 software.

Results of the performed analyses revealed the following parameters. The maximal value of the lateral displacement equal to 1.5 cm was obtained for the short side. Due to this parameter, it can be stated that the external façade should be viewed as critical because of stress concentrations. In terms of compressive stresses, the maximum values were found to be near the openings of the dome and the entrance wall with the maximum value close to 0.525 MPa. Tensile stresses were found to be concentrated around the dome openings and the top part of the entrance door. The latter was calculated as equal to 0.272 MPa. These parameters are critical from the perspective of cracks' formation and growth. Time-history analysis showed that shearing stresses exceeded the wall's characteristic shear strength. Results concerning displacement and stress values showed the possibility of the formation of damage within some areas.

Overall, the structural safety of the analyzed cistern under the impact of most of the 30 simulated earthquake scenarios was ensured. No significant damages to the structure of the cistern were reported. Nevertheless, repeated actions of earthquakes can increase stress levels and create favorable conditions for crack propagation. Consequently, problems related to cistern structure can arise. Such a situation can be associated with the extensive opening of the roof along the longitudinal direction.

On the basis of the received results, suggestions for strengthening the main weak spots of the cistern structure can be developed. It is suggested to add circumferential tension members or to use light and strong materials. Concerning wall openings, such actions as high-strength mortar injection and installing steel rods are recommended to reinforce walls, especially in critical areas like doors. The roof surface should be strengthened through installation of FRP strips/meshes.

It can be concluded that though the analyzed cistern is characterized by sufficient strength, strengthening is needed in the zones of high stress. It is necessary to accurately simulate joints of masonry historical structures during modeling to increase precision.

One of the distinctive features of this study is the focus on cisterns and their seismic performance. This paper contributes to the field through performing experimental and numerical studies of the dynamic behavior of one of cisterns under the action of earthquake forces. Based on the received results, the authors provide suggestions regarding retrofitting of such structures.

AUTHORSHIP CONTRIBUTIONS

Authors equally contributed to this work.

DATA AVAILABILITY STATEMENT

The authors confirm that the data that supports the findings of this study are available within the article. Raw data that support the finding of this study are available from the corresponding author, upon reasonable request.

CONFLICT OF INTEREST

The author declared no potential conflicts of interest with respect to the research, authorship, and/or publication of this article.

ETHICS

There are no ethical issues with the publication of this manuscript.

STATEMENT ON THE USE OF ARTIFICIAL INTELLIGENCE

Artificial intelligence was not used in the preparation of the article.

REFERENCES

[1] Bilxgin AR, Demirci D. Keçiborlu Senir'de bulunan Osmanlı dönemine ait üç sarnıç. Süleyman Demirel Üniversitesi Fen-Edebiyat Fakültesi Sosyal Bilimler Dergisi 2020;50:216–232.

[2] Güngör SS. Tarihi Yarımada'daki Roma ve Bizans dönemi sarnıçları. Stratejik ve Sosyal Araştırmalar Dergisi 2017;2:37–72. [CrossRef]

[3] Hasol D. "Sarnıç" maddesi. In: Ansiklopedik Mimarlık Sözlüğü. İstanbul: Y.E.M. Yayınları; 2008.

[4] Öter N. Muğla Sarnıçları [Master's thesis]. Konya: Selçuk Üniversitesi, Sosyal Bilimler Enstitüsü; 2008.

[5] Mays L, Antoniou GP, Angelakis AN. History of water cisterns: Legacies and lessons. Water 2013;5:1916–1940. [CrossRef]

[6] Bozkurt N. "Sarnıç" maddesi. In: Türkiye Diyanet Vakfı İslâm Ansiklopedisi. Vol. 36. İstanbul: Türkiye Diyanet Vakfı Yayınları; 2009. p. 158–159.

[7] Acar T. Beki ve Paşalar Köyü Özelinde Uşak Sarnıçları. The Journal of Academic Social Science Studies 2018;1:369–380. [CrossRef]

[8] Senthivel R, Lourenço PB. Finite element modelling of deformation characteristics of historical stone masonry shear walls. Eng Struct 2009;31:1930–1943. [CrossRef]

[9] Hrasnica M, Medic S. Seismic strengthening of stone masonry structures in Bosnia Herzegovina. In: Proceedings of the 15th World Conference on Earthquake Engineering. Lisbon; 2012. p. 12621–12628.

[10] Çelik T, Tanrıverdi Ş. Review of repair and strengthening studies in historical vaults. In: 10th International Conference on Engineering & Natural Sciences. 2021.

[11] Tanrıverdi Ş, Çelik T, Ural A, Fırat F. Kenet genişliğinin yığma taş bloklarının kayma davranışı üstündeki etkisinin incelenmesi. Düzce Üniversitesi Bilim ve Teknoloji Dergisi 2022;10:1811–1825.

[12] Vicente R, Lagomarsino S, Ferreira TM, Cattari S, Mendes da Silva JAR. Cultural heritage monuments and historical buildings: Conservation works and structural retrofitting. In: Strengthening and Retrofitting of Existing Structures. Springer; 2018. p. 25–57. [CrossRef]

[13] Tanrıverdi Ş, Çelik T. Farklı dolgu malzemeleri ile sabitlenen zıvanaların yığma taş blokların kayma dayanımına etkisi. Avrupa Bilim ve Teknoloji Dergisi 2021;25:347–354. [CrossRef]

[14] Ural A, Fırat FK, Kara ME, Çelik T, Tanrıverdi Ş. Damages to rubble stone masonry structures during the January 24, 2020, Sivrice (Elazığ) Earthquake in Turkey. Earthq Struct 2022;23:231–243.

[15] Brandão FDS, Diógenes A, Fernandes J, Mesquita E, Betti M. Seismic behavior assessment of a Brazilian heritage construction. Frattura ed Integrità Strutturale 2018;12:14–32. [CrossRef]

[16] Kumbasaroğlu A, Çelik A, Demir O, Turan AI, Yalçıner H. An assessment of the seismic performance of the historic Tigris Bridge. Open J Civ Eng 2019;9:230. [CrossRef]

[17] Salvatori L, Marra AM, Bartoli G, Spinelli P. Probabilistic seismic performance of masonry towers: General procedure and a simplified implementation. Eng Struct 2015;94:82–95. [CrossRef]

[18] Öztürk S. A study on the variations of recent seismicity in and around the Central Anatolian region of Turkey. Phys Earth Planet Inter 2020;301:106453. [CrossRef]

[19] Atmaca B, Demir S, Günaydın M, Altunışık AC, Hüsem M, Ateş Ş. Lessons learned from the past earthquakes on building performance in Turkey. J Struct Eng Appl Mech 2020;3:61–84. [CrossRef]

[20] Mutlu Ö, Şahin A. Investigating the effect of modeling approaches on earthquake behavior of historical masonry minarets-Bursa Grand Mosque case study. Sigma J Eng Nat Sci 2016;7:123–136.

[21] Ercan E, Arısoy B, Hökelekli E, Nuhoğlu A. Estimation of seismic damage propagation in a historical masonry minaret. Sigma J Eng Nat Sci 2017;35:647–666.

[22] Usta P, Bozdağ Ö. A new approximate method for earthquake behaviour of worship buildings. Civ Eng J 2019;5:2665–2685. [CrossRef]

[23] Mustafaraj E, Morina J. Structural assessment of Mehmed Pasha Hammam in Prizren. In: International Conference on Critical Thinking in Sustainable Rehabilitation and Risk Management of the Built Environment. Prizren, Kosovo; 2019. [CrossRef]

[24] Usta P, Bozdağ Ö. Earthquake analysis of historical Basdurak Mosque. Pamukkale Univ J Eng Sci 2021;27:244–250. [CrossRef]

[25] Aslay SE, Okuyucu D. Erzincan Değirmenliköy Kilisesi apsis hasarının teknik olarak araştırılması. Gazi Univ Muh Mim Fak Der 2020;35:387–402. [CrossRef]

[26] Hysenlliu M, Bidaj A, Bilgin H. Influence of material properties on the seismic response of masonry buildings. Res Eng Struct Mater 2020;6:425−437. [CrossRef]
[27] Yurdakul M, Yılmaz F, Artar M. Dynamic behaviour of Historical Bayburt Grand Mosque. Sigma J Eng Nat Sci 2020;11:1−11.
[28] Ahmadi HR, Mahdavi N, Bayat M. Applying adaptive pushover analysis to estimate incremental dynamic analysis curve. J Earthquake Tsunami 2020;14:2050016. [CrossRef]
[29] Ramaglia G, Lignola GP, Fabbrocino F, Prota A. Structural analysis of historical masonry churches: The case study of S. Giuseppe delle Scalze (Naples, Italy). Int J Masonry Res Innov 2021;6:472−501. [CrossRef]
[30] Doğangün A, Yön B, Onat O, Emin Öncü M, Sağıroğlu S. Seismicity of East Anatolian of Turkey and failures of infill walls induced by major earthquakes. J Earthquake Tsunami 2021;15:2150017. [CrossRef]
[31] Mohammedi L, Foufa AA, Zouaoui MC. Assessment of the seismic behaviour of heritage masonry buildings using numerical modelling: A study of Fernand Pouillon's Totem Tower in Algiers, Algeria. J Build Eng 2021;38:102183. [CrossRef]
[32] Demir S, Günaydin M, Atmaca B, Altunişik AC, Hüsem M, Adanur S. Performance evaluation of reinforced concrete buildings during the Sivrice-Elazığ earthquake (Mw=6.8, January 24, 2020) in accordance with Turkish Earthquake Code. J Earthquake Tsunami 2021;15:2150018. [CrossRef]
[33] Çelik T, Tanrıverdi Ş. Review of repair and strengthening studies in historical vaults. In: 10th International Conference on Engineering & Natural Sciences. 2021. p. 298−304.
[34] Ural A, Çelik T. Gaziantep Nizip Tahtani (Leylek) Cami yapısal analiz ve değerlendirmesi. Uludağ Univ Müh Fak Derg 2021;26:79−96. [CrossRef]
[35] Altunişik AC, Atmaca B, Kartal ME, Günaydin M, Demir S, Uluşan A. Assessment of structural damage following the October 30, 2020 Aegean Sea earthquake and tsunami. J Earthquake Tsunami 2021;15:2150029. [CrossRef]
[36] Fuzhang W, Imtiaz A, Hijaz A, Alsulami MD, Alimgeer KS, Cesarano C, et al. Meshless method based on RBFs for solving three-dimensional multi-term time fractional PDEs arising in engineering phenomena. J King Saud Univ Sci 2021;33:101650. [CrossRef]
[37] Pouraminian M. Multi-hazard reliability assessment of historical brick minarets. J Build Pathol Rehabil 2022;7:10. [CrossRef]
[38] Mohammed WW, Cesarano C. The soliton solutions for the (4+1)-dimensional stochastic Fokas equation. Math Methods Appl Sci 2023;46:7589−7597. [CrossRef]
[39] Schiavoni M, Giordano E, Roscini F, Clementi F. Numerical modeling of a majestic masonry structure: A comparison of advanced techniques. Eng Fail Anal 2023;149:107293. [CrossRef]
[40] Sacco GLS, Ferrero C, Battini C, Calderini C. Combined use of deformation and structural analysis for the structural damage assessment of heritage buildings: A case study in the Liguria region (Italy). Eng Fail Anal 2023;147:107154. [CrossRef]
[41] Romero-Sánchez E, Morales-Esteban A, Bento R, Navarro-Casas J. Numerical modelling for the seismic assessment of complex masonry heritage buildings: The case study of the Giralda tower. Bull Earthq Eng 2023;21:4669−4701. [CrossRef]
[42] Sinaei S, Izadi Zaman Abadi E, Hoseini SJ. Failure analysis of skewed Persian brick masonry barrel vaults: Experimental and numerical study. J Perform Constr Facil 2023;37:04023057. [CrossRef]
[43] Hassani Sokhtesaraei M, Ghassemieh M, Mirghaderi SR. Proposing a set of far-field records for time history analysis in Tehran city and comparison with FEMA-P695 set records. J Earthq Tsunami 2023;17:2250017. [CrossRef]
[44] Aykanat B, Ertürk E, Altunışık AC, Aslan ME. Field investigation on reinforced concrete and masonry buildings damages after November 23, 2022 Gölyaka (Düzce) earthquake. J Earthq Tsunami 2023;17:2350010. [CrossRef]
[45] Güner Y, Nuhoğlu A. Development and application of the truss method on masonry walls to determine the in-plane behavior: A parametric study. Sigma J Eng Nat Sci 2023;42:1542−1554. [CrossRef]
[46] Altunisik AC, Arslan ME, Kahya V, Aslan B, Sezdirmez T, Dok G. Field observations and damage evaluation in reinforced concrete buildings after the February 6th, 2023, Kahramanmaras-Turkiye earthquakes. J Earthq Tsunami 2023;17:2350024. [CrossRef]
[47] Sevim B, Ayvaz Y, Akbulut S, Aydiner M, Uzun S, Ari A. Seismic performance and damage evaluation of reinforced concrete structures based on field investigation made after February 6, 2023, Kahramanmaraş Earthquakes. J Earthq Tsunami 2023;18:2350032. [CrossRef]
[48] Hacıefendioğlu K, Özgan K, Adanur S, Altunışık AC, Demirer B, Günaydın M. Estimation of damage levels in masonry structures following earthquake impact using deep learning-based segmentation method. J Earthq Tsunami 2024;18:2450006. [CrossRef]
[49] Cırak IF. Yığma yapılarda oluşan hasarlar, nedenleri ve öneriler. SDU Int Technol Sci 2011;3:55−60.
[50] Turkish Standards Institution. TS EN 1926: Natural stone test methods-determination of uniaxial compressive strength. Ankara: Turkish Standards Institution; 2007.
[51] Gönen S, Soyöz S. Seismic analysis of a masonry arch bridge using multiple methodologies. Eng Struct 2021;226:111354. [CrossRef]

[52] Çoban K. Determination of the dynamic performance of historical Bayburt Yakutiye (Yeni) mosque [Master's thesis]. Bayburt: Bayburt University; 2018.
[53] Ministry of Public Works and Settlement. Turkish Building Earthquake Code (TBEC). Ankara: Ministry of Public Works and Settlement; 2019.
[54] Artar M, Coban K, Yurdakul M, Can O, Yilmaz F, Yildiz MB. Investigation on seismic isolation retrofit of a historical masonry structure. Earthq Struct 2019;16:501–512.
[55] Computers and Structures Inc. SAP2000: Integrated finite element analysis and design of structures (Version 23.1.0) [Software]. Berkeley: Computers and Structures Inc.; 2021.
[56] Caicedo D, Karimzadeh S, Bernardo V, Lourenço PB. Selection and scaling approaches of earthquake time-series for structural engineering applications: A state-of-the-art review. Arch Comput Methods Eng 2023;30:4411–4441.
[57] Pacific Earthquake Engineering Research Center (PEER). Ground motion database. 2021. Available from: https://ngawest2.berkeley.edu/
[58] Pardalopoulos SI, Pantazopoulou SJ. Methodology for practical seismic assessment of unreinforced masonry buildings with historical value. Earthq Eng Struct Dyn 2017;46:2793–2810. [CrossRef]
[59] Lagomarsino S, Cattari S. PERPETUATE guidelines for seismic performance-based assessment of cultural heritage masonry structures. Bull Earthq Eng 2015;13:13–47. [CrossRef]
[60] Halder L, Dutta SC, Sharma RP. Damage study and seismic vulnerability assessment of existing masonry buildings in Northeast India. J Build Eng 2020;29:101190. [CrossRef]
[61] Sarhosis V, Dais D, Smyrou E, Bal IE, Drougkas A. Quantification of damage evolution in masonry walls subjected to induced seismicity. Eng Struct 2021;243:112529. [CrossRef]
[62] Mazza F, Donnici A. In-plane-out-of-plane single and mutual interaction of masonry infills in the nonlinear seismic analysis of RC framed structures. Eng Struct 2022;257:114076. [CrossRef]
[63] Demirel IO. A nonlinear equivalent frame model for displacement-based analysis of unreinforced brick masonry buildings [Master's thesis]. Ankara: Middle East Technical University; 2010.
[64] Franklin SG, Abrams DP, Klinger RE, Schuller MP. Performance testing for seismic rehabilitation of URM buildings. Earthq Spectra 2001;17:583–606.
[65] Bosiljkov V, Uranjek M, Zarnic R, Bokan-Bosiljkov V. Evaluation of masonry properties from combined testing of small specimens and wallets. Mater Struct 2008;41:1333–1355.
[66] Alcocer SM, Arias JG, Varela-Rivera J. Seismic behavior of confined masonry walls. J Struct Eng 2004;130:588–599.
[67] Salonikios T, Theodoulidis N, Zacharopoulou G. Seismic response evaluation of monuments based on ambient vibrations: The case studies of a Byzantine Basilica and an Ottoman bath in Thessaloniki (Greece). J Seismol 2020;24:777–802. [CrossRef]